

Arab Academy for Science, Technology and Maritime

Transport

College of Engineering and Technology

Mechanical Engineering Department

B. Sc. Final Year Project

New Savonius Wind Turbine Design

Presented By:

Mahmoud ahmed Mohamed aboubakr Ali magdy

Ahmed tamer selim Mohamed Samir

Maged mohamed

Supervised By:

Prof. Rola Afify

Prof. Ahmed Samir

Prof Walid Ghoneim

Declaration

I hereby certify that this report, which I now submit for assessment on the programme of study leading to the award of Bachelor of Science in Mechanical Engineering, is all my own work and contains no Plagiarism. By submitting this report, I agree to the following terms:

Any text, diagrams or other material copied from other sources (including, but not

limited to, books, journals, and the internet) have been clearly acknowledged and cited

followed by the reference number used; either in the text or in a footnote/endnote. The

details of the used references that are listed at the end of the report are confirming to

the referencing style dictated by the final year project template and are, to my knowledge, accurate and complete.

I have read the sections on referencing and plagiarism in the final year project template. I understand that plagiarism can lead to a reduced or fail grade, in serious cases, for the Graduation Project course.

Student Name: Mahmoud ahmed aboubakr	Student Name: Ali magdy
Registration Number: 17101037	Registration Number: 17100460
Signed:	Signed:
Date: 6-7-2022	Date: 6-7-2022
Student Name: Ahmed tamer	Student Name: Maged mohamed
Registration Number: 17101035 R	egistration Number:17101579
Signed:	Signed:

Date: 6-7-2022

Student Name: Mohamed Samir	
Registration Number: 17101220	
Signed:	

ACKNOWLEDGMENT

Primarily we would like to thank God for being able to complete this project with success. Then we would like to thank dr. Rola Afify, whose valuable guidance has been the success, her suggestions and instructions has served as the major contribution towards the completion of the project, we also would like to thank dr. ahmed samir who always directed us toward the information we needed to understand the concept and idea of this project.

Then we would like to thank our parents and friends who have helped us with their valuable suggestions and guidance has been helpful in various phases of the completion of the project.

Abstract

Renewable energy has been utilized by humans ever—since the dawn of the civilization in a try to take advantage of nature's resources to make life better. The many forms of renewable energy comes mainly from the sun the heats the planet, subsequently moves the air to make winds that moves the seas the rivers creating all forms of six main renewable energy resources.

Wind energy is a form of renewable that is available everywhere on the planet and can be harnessed in many ways and currently contributes in a huge percentage of overall renewable energy production worldwide. Our aim is manufacture one of wind energy's harnessing equipment and try to modify it for better performance and try to eliminate drawbacks that exists in traditional equipment through various experiments.

Table of Content

Contents

1.1 Introduction2
1.1.1 Vertical axis wind turbine2
1.1.2 Advantage of VAWT
1.1.3 Disadvantage of VAWT3
1.2 Savonius turbine3
1.2.1 Power calculation4
1.3 Design of VAWT5
1.3.1 Savonius rotor design5
1.4 Component of savonius turbine5
1.4.1 Guide wire6
1.4.2 Hub6
1.4.3 Rotor6
1.4.4 Rotor blades6
1.4.5 Shaft7

1.4.6 Electrical braking7	
1.4.7 Mechanical braking7	
1.4.8 Gearbox7	
1.4.9 Generator8	
1.5 Effieciency8	
1.5.1 Working principle8	
1.5.2 Parameters that effect the performance of savonuis wind turbine.9	
1.5.2.1 Effect of blades number9	
1.5.2.2 Effect of aspect ratio	
1.5.2.3 Effect of end plates10	
1.6 Application11	
1.6.1 Buildings11	
1.6.2 Provide local electricity12	
1.6.3 Power cellular communication towers	
1.7.1 Mechanism13	
1.7.2 Shapes of blades	.15
1.7.3 Expermental setup	16
1.8 Torque of savonuis turbine	16
1.8.1 Mechanism of torque	17
1.8.2 Summary	19
1.9 Power and rotational speed	19
1.9.1 tip speed ratio	20
1.9.2 CP	20
2.1 Usfel information	.25
2.1.1 Blade width	25
2.1.2 Tip speed ratio	25
2.1.3 Power and torque from blades	26
2.1.4 Betz law	26
2.2. Force analysis on the turbine parts	26
2.3.Stress analysis	27
2.3.1 Stresses on turbine rodes	27

2.3.2 Direct shear due to weight	27
2.3.3 Torsion due to weight	27
2.3.4 Compression stress due to wind force	27
2.3.5 Material selection for the blades	28
2.3.6 Tension stress due to centrifugal force	28
2.3.7 Bending stress due to weight	28
2.3.8 Direct shear due to weight	29
2.3.9 Direct shear due to centrifugal	29
2.3.10 Bearing stress on rod	29
2.4. Design of shaft	30
2.4.1Shaft material	30
2.4.2 Design based on distortion	32
2.4.3 Design based on rigidity	32
2.4.4 Design based on fatigue	32
2.4.5 Design based on ASME formula of ductile material	33
2.5 Selection of bearing	36
2.5.2 Static load bearing	36
2.5.3 Check for dynamic load	37
2.5.4 Dynamic load calculation	37
3.1 Expermental study	40
3.2Expermental setup	40
3.3Equipment	42
3.3.1 Wind tunnel	42
3.3.2 Pitot static probe	42
3.3.3 Laod cell	42
3.3.4 Arduino	43
3.3.5 Blades design	44
3.3.6 Shaft design	45
3.3.7 Additional artilon design	44
3.4 Data reduction	51
3.5 Experiments	52

3.5.1 Experiment1	52
4.1 New design results	54
4.2 Traditional design results	54
4.3 RPM readings	.55
4.4 Torque readings	55
4.5 Power readings	56
5.1 Conclusion	58

List of figures

Figure 1-1:The world's tallest vertical-axis wind turbine	2
Figure 1-2: Schematic drawing of a two-scoop Savonius turbine	4
Figure 1-3: savonius style vawt	5
Figure 1-4: Savonius turbine blades effect	9
Figure 1-5: Effect of number of blades	9
Figure 1-6: Effect of aspect ratio	10
Figure 1-7: Effect of end plates	11

Figure 1-8: Savonius turbine
Figure1-9:power cellular communication towers
Figure 1-10: Blade geometry14
Figure 1-11: Photographic view
Figure 1-12 : starting torque
Figure 1-13 : Before reducing reference angle
Figure 1-14: After reducing
Figure 1-15: Max. torque less than two
blades18
Figure 1-16: Relation between wind speed and
rpm22
rpm22 Figure 1-17: Relation between wind speed and power22
Figure 1-17: Relation between wind speed and power22
Figure 1-17: Relation between wind speed and power
Figure 1-17: Relation between wind speed and power
Figure 1-17: Relation between wind speed and power

Figure 3.7 Thermo Anemometer	
Figure 3.8 Image of the electric panel of the setup47	
Figure 3.9. Side view of the old design48	
Figure 3.10. Side view of the new design49	
Figure 3.11 Artylon part 150	
Figure 3.12 Artylon part 250	
Figure 4.13 RPM Readings55	
Figure 4.14 Torque Readings55	5
Figure 4.15 Power Readings56	
List of tables	
Table 4.1 New design results	54
Table 4.2 traditional design results5	4

Chapter One Introduction

Chapter one

1. INTRODUCTION

1.1 INTRODUCTION

1.1.1 vertical axis wind turbines

A vertical-axis wind turbine (VAWT) is a type of wind turbine where the main rotor shaft is set transverse to the wind (but not necessarily vertically) while the main components are located at the base of the turbine. This arrangement allows the generator and gearbox to be located close to the ground, facilitating service and repair. VAWTs do not need to be pointed into the wind which removes the need for wind-sensing, A vertical axis Wind turbines are built to be both cost-effective and practical, as well as silent and efficient. A wind turbine directs air into a hub, which converts it into electricity. Rotational momentum spins the air that travels between the blades of the wind turbine into the generator.[1]



Figure 1-1:The world's tallest vertical-axis wind turbine, in Cap-Chat, Quebec

There are two types of VAWTs first one named Darrieus Wind Turbine and it is commonly known as an "Eggbeater" turbine. It was invented by Georges Darrieus in 1931. A Darrieus is a high speed, low torque machine suitable for generating alternating current (AC) electricity. Darrieus generally require manual push therefore some external power source to start turning as the starting torque is very low. Darrieus has two vertically oriented blades revolving around a vertical shaft. Second type called Savonius vertical-axis wind turbine is a slow rotating, high torque machine with two or more scoops and are used in high-reliability lowefficiency power turbines. Most wind turbines use lift generated by airfoil-shaped blades to drive a rotor, the Savonius uses drag and therefore cannot rotate faster than the approaching wind speed.[2]

1.1.2 Advantages of VAWT

- 1. You do not need any mechanisms in order to operate the wind turbine
- 2. Lower wind startup speed
- 3. The main advantage of VAWT is it does not need to be pointed towards the wind to be effective.
- 4. You can build your wind turbine close to the ground so if you do not have a suitable rooftop for placement, or if you live where there are hills, ridges, etc. that prohibit the flow of air, they work wonderfully for your needs.

1.1.3 Disadvantages of VAWT

- 1. You are unable to take advantage of the wind speeds that occur at higher levels.
- 2. VAWT's are very difficult to erect on towers, which means they are installed on base, such as ground or building.[3]

1.2 SAVONIUS TURBINE

The Savonius wind turbine was invented by the Sigurd Johannes Savonius in 1922, it is one of the type of vertival axis wind turbine (VAWT) use to converting the force of the wind into torque.[4]

The Savonius turbine is one of the simplest turbines. Aerodynamically, it is a drag-type device, consisting of two or three scoops. Looking down on the rotor from above, a twoscoop machine might resemble the letter "S" in cross section. Because of the curvature, the scoops experience less drag when moving against the wind than when moving with the wind. The differential drag causes the Savonius turbine to spin. Because they are drag-type devices, Savonius turbines extract much less of the wind's power than other similarly-sized lift-type turbines. In practice, much of the swept area of a Savonius rotor may be near the ground if it has a short mount without an extended post, making the overall energy extraction less effective due to the lower wind speeds found at lower heights so The basic principle is based on the difference of the drag force between the convex and the concave parts of the rotor blades when they rotate around a vertical shaft. Thus, drag force is the main driving force of the savonius rotor.

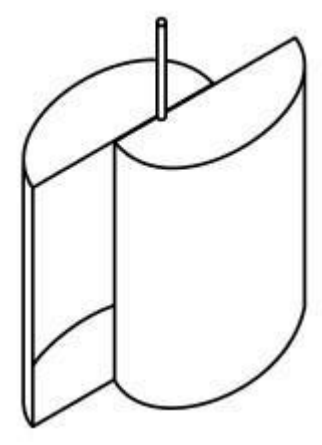


Figure 1-2: Schematic drawing of a two-scoop Savonius turbine

1.2.1 Power calculation

Aaccording to betz law the maximum power that can be extract from a rotor is

1.3 DESIGN OF VAWT

1.3.1 Savonius Rotor Design

the design of rotor is formed by dividing a cylinder into half, along its central axis and relocating the two semi-cylindrical surfaces sideways. This shape is akin to "S" when viewed from top. These type of rotors may be of two, three or higher bladed systems and can be used in single- or multi-staged arrangements. The working principle is based on the difference of the drag force between the convex and the concave parts of the rotor blades when they rotate around [6]

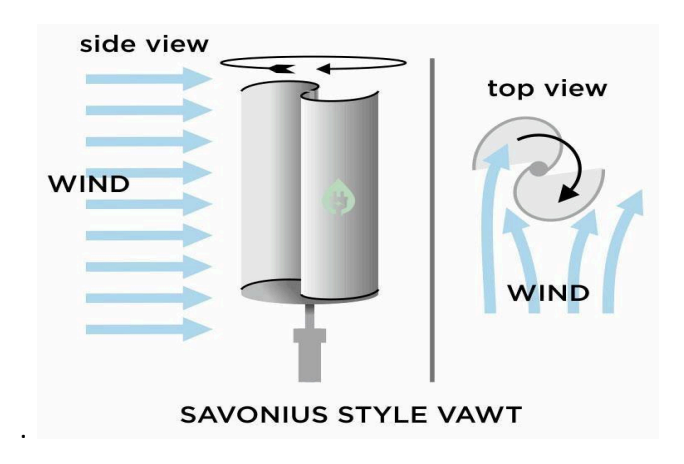


Figure 1-3: savonius style vawt

1.4 COMPONENTS OF SAVONIUS TURBINE

- Guide wire
- Hub
- Rotor
- Blades
- Shaft Brakes

- Gear
- Generator
- Base

1.4.1 Guide wire

Vertical axis wind turbine normally needs guide wire to keep the rotor shaft in a fixed position and maximised possible mechanical vibration.

1.4.2 Hub

The hub is the centre of the rotor to which the rotor blades are attached. Cast iron or cast steel is most often used. In VAWT there are two hibs upper and lower because blades are attached at two points.

1.4.3 Rotor

The rotor is the heart of a wind turbine and consists of multiple rotor blades attached to a hub. It is the turbine component responsible for collecting the energy present in the wind and transforming this energy into mechanical motion. As the overall diameter of the rotor design increases, the amount of energy that the rotor can extract from the wind increases as well. Therefore, turbines are often designed around a certain diameter rotor and the predicted energy that can be drawn from the wind.

1.4.4 Rotor blades

Rotor blades are a crucial and basic part of a wind turbine. they are mainly made of aluminium, fibber glass or carbon fibber because they provide batter strength to weight ratio. The design of the individual blades also affects the overall design of the rotor. Rotor blades take the energy out of the wind; they "capture" the wind and

convert its kinetic energy into the rotation of the hub. there are two types of blades use in VAWT

Drag force type blades (savonius wind turbine) Lift force type blades (Darrieus and giromill wind turbine)

1.4.5 Shaft

The shaft is the part that gets turned by the turbine blades. It in turn is connected to the generator within the main housing

1.4.6 Electrical braking

Braking of a small wind turbine can also be done by dumping energy from the generator into a resistor bank, converting the kinetic energy of the turbine rotation into heat. This method is useful if the kinetic load on the generator is suddenly reduced or is too small to keep the turbine speed within its allowed limit.

Cyclically braking causes the blades to slow down, which increases the stalling effect, reducing the efficiency of the blades. This way, the turbine's rotation can be kept at a safe speed in faster winds while maintaining (nominal) power output. This method is usually not applied on large grid-connected wind turbines.

1.4.7 Mechanical braking

A mechanical brake is normally placed on the high speed shaft between the gearbox and the generator, but there are some turbine in which the brake is mounted on the low speed shaft between the turbine and gear box

A mechanical drum brake or disk brake is use to stop turbine in emergency situation such as extreme gust events or over speed. This brake is also used to hold the turbine at rest for maintenance as a secondary mean, primarily mean being the rotor lock system. Such brakes are usually applied only after blade furling and electromagnetic braking have reduced the turbine speed generally 1 or 2 rotor RPM, as the mechanical brakes can create a fire inside the nacelle if used to stop the turbine from full speed. Also the load on turbine increases if brake is applied on

rated RPM. These kind of mechanical brake are driven by hydraulic systems and connected to main control box.

1.4.8 Gear box

The main function of the gear box is to take low rotational speed from shaft and increase it to increase the rotational speed of the generator. Among the types of gear stages are the plantary, helical, parallel shaft, spur and worm types. Two or more gear types may be combined in multiple stages. they are made up of aluminum alloys, stainless steel and cost iron

1.4.9 Generator

The conversion of rotational mechanical energy to electrical energy is performed by generator. Different types of generator have been used in wind energy system over the years. For large, commercial size horizontal-axis wind turbines, the generator is mounted in a nacelle at the top of a tower, behind the hub of the turbine rotor. Typically wind turbines generate electricity through asynchronous machines that are directly connected with the electricity grid. Usually the rotational speed of the wind turbine is slower than the equivalent rotation speed of the electrical network - typical rotation speeds for wind generators are 5-20 rpm while a directly connected machine will have an electrical speed between 750-3600 rpm. Therefore, a gearbox is inserted between the rotor hub and the generator. This also reduces the generator cost and weight [7]

1.5 EFFIECIENCY

1.5.1 Working principle

The Savonius wind turbine is a simple vertical axis device having a shape of half-cylindrical parts attached to the opposite sides of a vertical shaft (for two-bladed arrangement) and operate on the drag force, so it can't rotate faster than the wind speed. This means that the tip speed ratio is equal to 1 or

smaller. as the wind blows into the structure and comes into contact with the opposite faced surfaces (one convex and other concave), two different forces (drag and lift) are exerted on those two surfaces. The basic principle is based on the difference of the drag force between the convex and the concave parts of the rotor blades when they rotate around a vertical shaft. Thus, drag force is the main driving force of the savonius rotor [8]

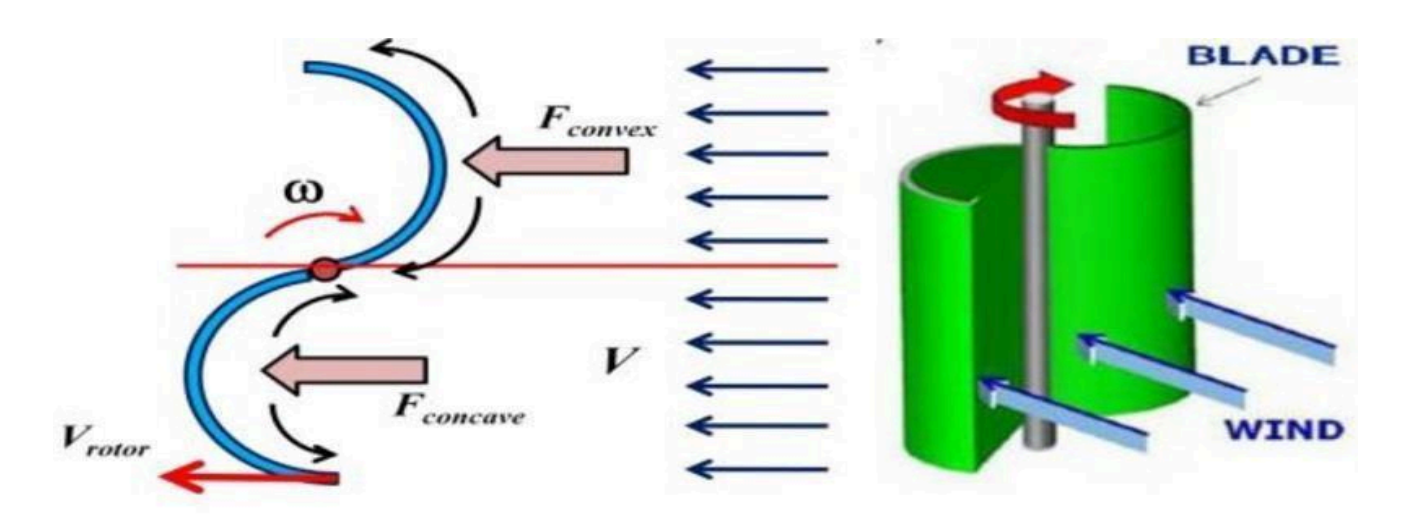


Figure 1-4: Savonius turbine blades effect

1.5.2 Parameters that affect the performance of Savonius wind turbine

1.5.2.1 Effect of blades number

The number of blades have an important impact in the rotor's performance the

two blades Savonius wind turbine is more efficient, it has higher power coefficient under the same test condition than that of three blades Savonius wind turbine. [9]

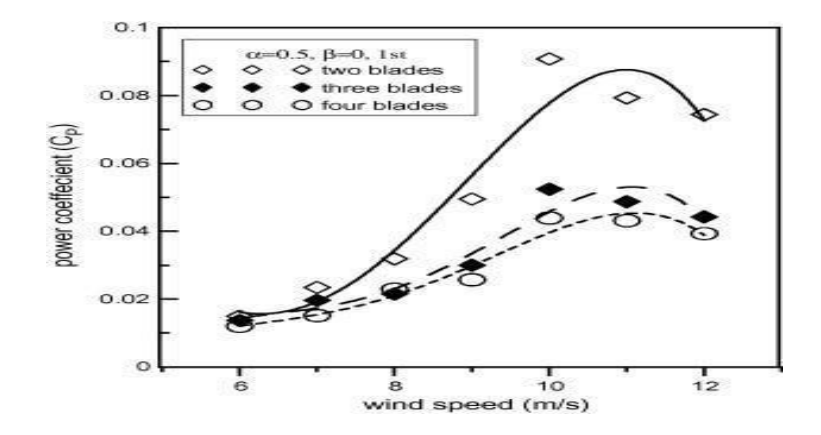


Figure 1-5: Effect of number of blades

1.5.2.2 Effect of Aspect Ratio

The aerodynamic performance of the Savonius rotor depends strongly on the aspect ratio .

Different rotors with aspect ratios from 0.5 to 5 are studied experimentally at constant values of the other studied parameters. [9]

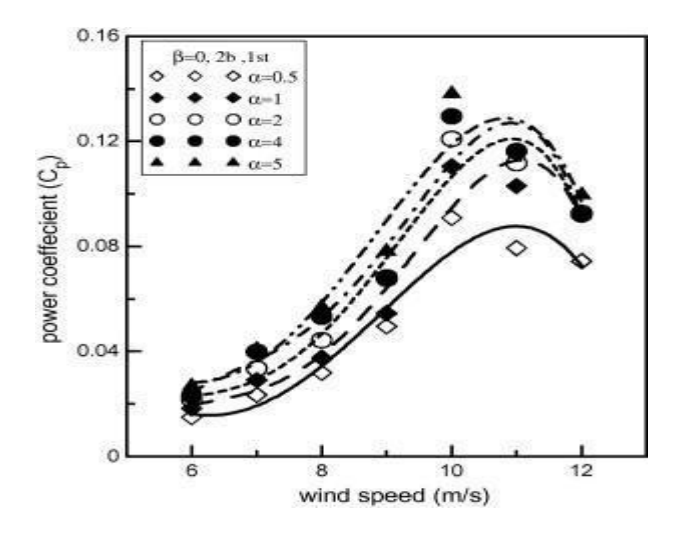


Figure 1-6: Effect of aspect ratio

1.5.2.3 Effect of end plates

rotors with and without end plates are tested at constant values of other considered parameters. Variation in mechanical power with wind speed for rotors with and

without end plates is given in Fig. . Rotors with end plates give higher mechanical power than rotors without end plates.[9]

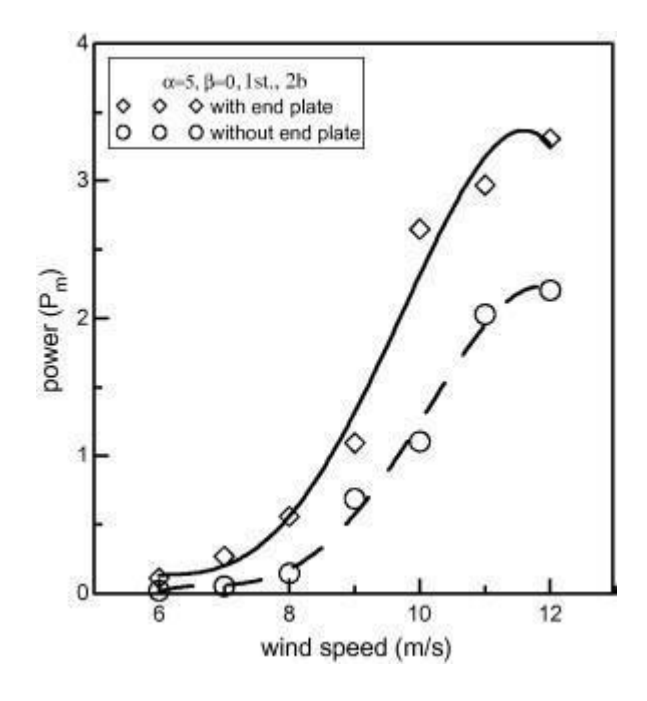


Figure 1-7: Effect of end plates

1.6 APPLICATIONS

1.6.1 Building

Turbine is attached to a building and is used to provide local electricity. Often, buildings have large equipment such as heating, ventilation, and air-conditioning (HVAC) units which create obstructions to airflow or to the positioning of the turbine. A VAWT can be placed in more confined spaces than a HAWT. [10]



Figure 1-8: Savonius turbine

1.6.2 Provide local electricity

It provides local electricity for residents of remote villages in the developing world. Small, robust VAWT systems with battery storage capability enable the intermittent generation and storage of power which can be used for small electronics, charging of cellular phones, or lighting.

1.6.3 Power cellular communication towers

Another very promising application for VAWTs is to power cellular communication towers. Around the world, growth in cellular communication is strong with many countries bypassing more traditional land-line phone networks. A cellular communication network requires adequate coverage for its users. Consequently, a sufficient number of communication towers with antennas are needed for this coverage. The typical power requirements are 1-3 kW for cell-phone electronics associated with a modern tower. In some instances, this energy is provided by VAWT.[10]



Figure 1-9: power cellular communication towers

1.7- TYPES OF SAVINOUS TURBINE:

1.7.1-Mechanism

The efficiency of Savonius turbines is typically 15 to 20%, which is less than half that of HAWTs. Drag-driven devices are commonly referred to as Savonius turbines. The lift force also contributes to the overall torque generation at low angles of attack. It can go beyond the purely drag-driven machines' power coefficient (CP) limit of 8%. The researchers used a neural network to model turbine performance that varies depending on blade configuration The power coefficient of a turbine increased by up to 123 percent for two blade models and 150 percent for three blade models when it was surrounded by a guide box. To simulate turbine performance as it varies with Savonius blade configuration. The proposed configuration of Al-Faruk et al. [1]

was investigated experimentally in order to determine the effects of geometrical parameters on its performance in the current study. Several physical parameters, such as blade overlap ratio, blade arc angle, and the diameter of the swirling chamber's hot air inlet, are taken into account to determine their effects on aerodynamics performance in terms of coefficient of power and coefficient of torque. The current experimental setup allows performance evaluations of the new swirling type Savonius rotor (for ease of calling, for example). swirling Savonius rotor) and the traditional Savonius rotor. Savonius Turbine in a Swirl The swirling Savonius turbine is similar to the classic Savonius turbine, which consists of two identical semi-cylinder-like blades moving sideways and overlapping, as shown in "figure 1." The swirling Savonius turbine differs from a traditional Savonius turbine in that it has been modified. The inner tips of the half cylinders were extended further to construct the swirling chamber [1], which had a 180o blade angle. The extended angle () of the blades as shown in "figure 1" reduces the vortex chamber's air entrainment gap. The swirling chamber's hot air inlet is a circular hole in the bottom end plate with a diameter of d. Figure 1 shows the blade geometry on the swirling rotor's bottom end plate. The blade material is a light-weight, low-cost u-PVC pipe with a nominal diameter of 150 mm. The pipe's average outside diameter was 160 mm, and the average wall thickness was 3 mm. [11]

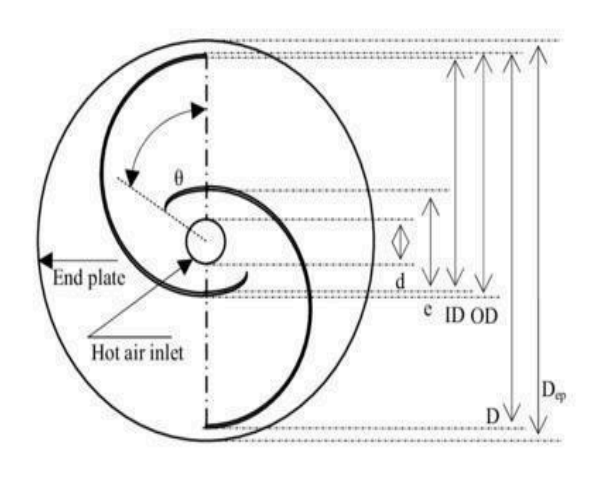


Figure 1-10: Blade geometry



Figure 1-11: Photographic view

1.7.2 Shape of blades

At the top and bottom ends of the blades, two circular end plates were used to connect them. To provide a clear top view of the turbine, the bottom end plate was made from 3 mm thick Aluminum sheet, and the top end plate was made from 3 mm thick Acrylic sheet with a hole in the centre. As shown in "figure 1," a circular hole with a diameter of 44 mm has been cut in the centre of the bottom end plate as the hot air inlet. The pipe was cut into two 1800 half cylinders and paired 100, 150, 200, and 300 slots, which were used to make various swirling Savonius type geometrical rotors. After you've decided on the blade geometry's dimensions, you can move on to the next step. The 1800 half cylinders were first joined with the end plates using a strong adhesive, such as blade overlap ratio and blade arc angle. To create the swirling rotor blades, the inner tip of the blades were extended by connecting the required arc angled slots with the 1800 blades. The components were dismantled and reassembled for subsequent experiments after completing experiments with the same rotor. The diameter (d) of the swirl chamber was changed by placing aluminium sheets on top of the hot air inlet. Six washers and bolts were used to connect the bottom end plate of the turbine to the end flange of an Aluminum hollow shaft (44 mm inner diameter and 50 mm length). The rotor was then inserted into the test bench's ball bearing. Rotor replacement was made easier with the use of a flanged hollow shaft. The weight of the rotor was further reduced due to the use of only one bearing and the absence of a top shaft. The bearing mechanism is moved closer to the centre of rotation, which reduces the possibility of peripheral mass problems and vibrations caused by an unbalanced assembly. the bearing housing that has been built The warm air from the hot air chamber is carried to the bottom of the hollow shaft via a stainless steel pipe with a 50 mm outer diameter and a 44 mm inner diameter. Finally, hot air exits the chimney through the hollow shaft and enters the turbine. To measure the temperature of the warm air entering the rotor's swirling chamber, a K-type thermocouple was inserted through a hole at the top end of the chimney.[12]

1.7.3 EXPRIMENTAL SET-UP

A structural test bench, which houses the swirling Savonius rotor and the hot air generation chamber, as well as an industrial pedestal fan and measurement devices, make up the experimental setup. Three speed settings and height adjustment are available on a 750 mm diameter industrial pedestal fan used in this project. The rotor and a few measuring devices were placed on top of the table, while the heating chamber was placed beneath it. The rotor was supported by a single low friction 50 mm bore diameter ball bearing that was rigidly bolted to the table when the rotor was stopped. The dynamometer's spring balance readings, dead weights, and maximum steady state rotational speeds of the rotor were all recorded and used to calculate the transmitted load/torque and brake power. Finally, the performance parameters were examined as a function of the tip speed ratio. The coefficient of power (CP) and coefficient of torque (Ct), which are usually calculated as a function of the dimensionless tip speed ratio (), are two dimensionless performance parameters commonly used in the aerodynamics of wind turbines. The following are the definitions: Cp =P12pDHU3, Ct =

T14pD2HU2 and $\gamma = \omega D2U$ where ρ is the air density, U wind velocity, P mechanical power, H rotor height, and D rotor diameter.[12]

1.8 Torque of savionus turbine

Using a Futek torque sensor, the starting torque was measured. The rotor will be aligned at a reference point during each measurement Following the completion of the measurement, the rotor will be rotated 10 degrees counterclockwise to measure the starting torque at the next azimuthal angle. This cycle repeats itself until the revolution is complete. At a wind speed of 4.45 m/s, this test was conducted. At 4.45 mph, the rotor's starting behaviour was also observed. The tunnel will be turned on and the rotor will be kept still in this type of test. The rotor was released and its rotational speed was recorded at a sampling rate of 1 Hz after the wind speed stabilised. By applying a known load to the other end of the torque sensor,

the Futek sensor was also used to measure power .The strain gauge detects a net torque exerted by the rotor to spin the load, as well as a rotational speed at which the entire turbine rotates at the same time, with this load. The product of two measured quantities equals the turbine's power.[13]

1.8.1 Mechanism of torque

The starting torque of the two-bladed rotors as a function of the azimuthal angle are presented in figure 1-12.

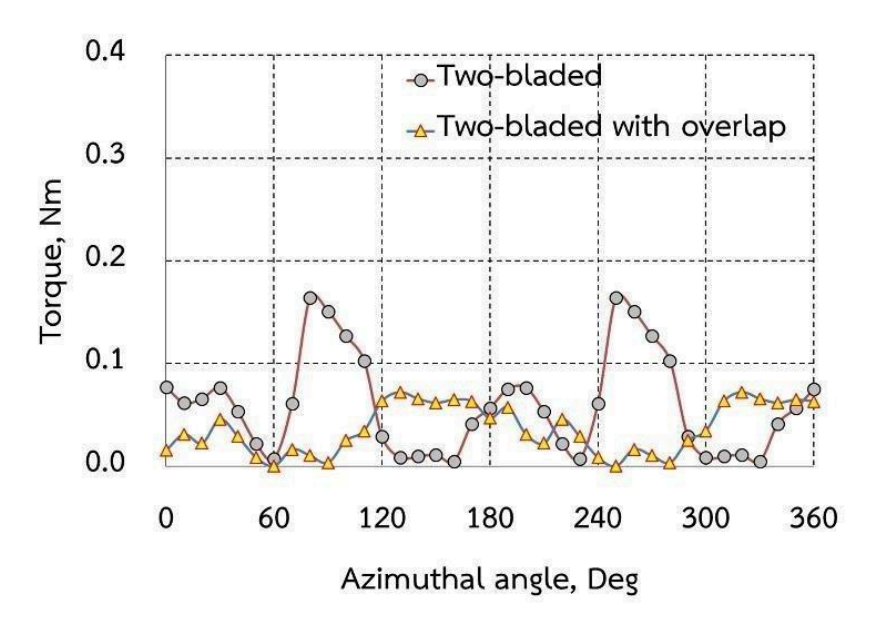
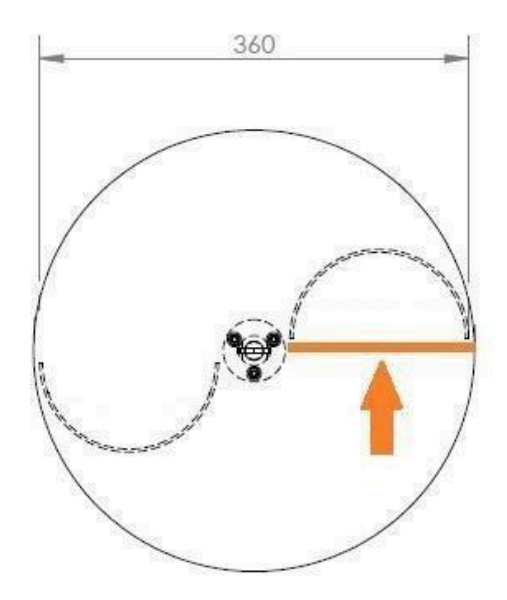


Figure 1-12: starting torque

The overlap ratio has a significant impact on the torque distribution over the azimuthal angle, as shown in figure. The amount of torque at the reference angle is reduced to 0.015 Nm, down from 0.077 Nm, and this is thought to be the result of a smaller swept area, which reduces the rotor blade's effective area As a result, torque is reduced over the azimuthal range. Following that, the average torque is reduced to 0.039 Nm.[13]



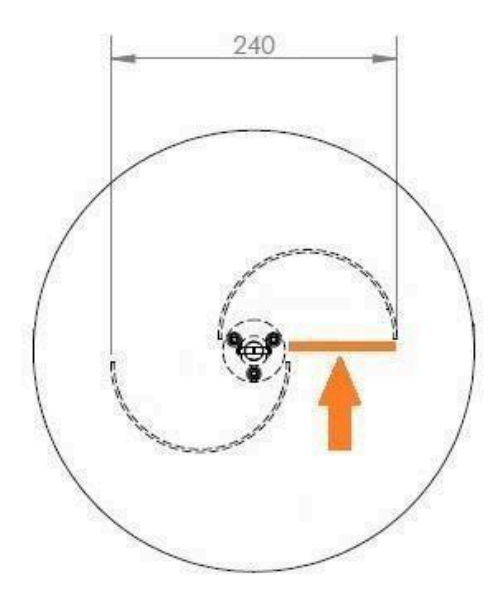


Figure 1-13 : Before reducing reference angle

Figure 1-14: After reducing

The peak torque is less noticeable in three-bladed configurations At the reference point, the torque value for a three-bladed rotor without the overlap angle is about 0.027 Nm. It's worth noting that this stating torque is lower than the two-bladed one, which is thought to be due to blade interference. The maximum torque is reduced to 0.1 Nm, with an average torque of 0.076 Nm per revolution. The nearby blade will divert the airflow in this case. this effect increases as the blade moves further away from the incoming wind. Despite the fact that the two-bladed configuration can produce more torque, It is subjected to pulsation on a regular basis, resulting in bearing failure.

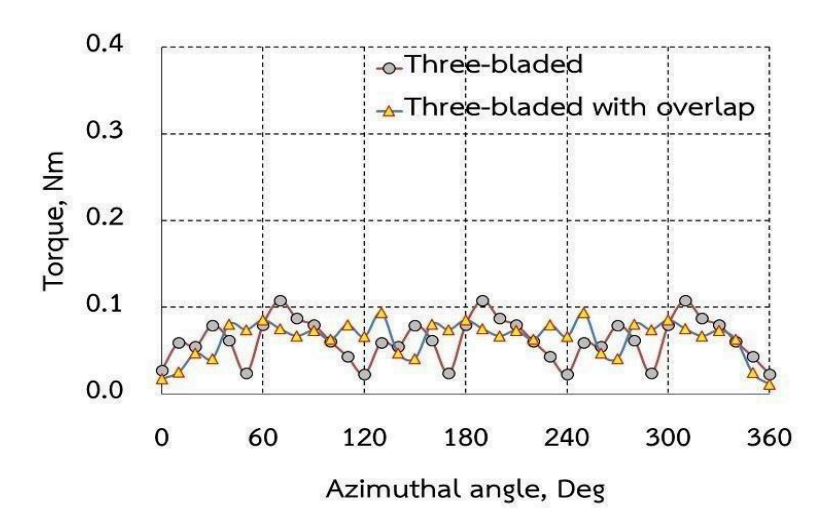


Figure 1-15: Max. torque less than two blades

The torque distributions of the two- and three-bladed rotors in figures show that, while the three-bladed rotor's maximum torque is lower than the two-bladed case, its torque distribution is comparatively flat and does not experience a large drop to a nearly zero value at azimuthal angles between 130 and 180, as the two-bladed cases do. The overlap ratio is used to reduce the rotor's overall torque generation once more.[13]

1.8.2 Summary:

The number of blades has a significant impact on the initial characteristics. Both with and without the overlap ratio, a three-bladed rotor will always produce more continuous torque. Because the swept area is smaller, the overlap ratio reduces the torque generated by the turbine and thus its starting ability. The use of lightweight materials is beneficial and the optimal configuration might be different if different materials are used. The three-bladed rotor with the lowest overlap ratio has the best starting capability and power extraction performance of all the rotors tested.

1.9 POWER & ROTATIONAL SPEED:

According to Bet'z law, the maximum power that is possible to extract from a rotor is $Pmax = (16/27)(1/2)(\rho.h.d.v^3)$, where ρ is the density of air, h and d are the height and diameter of the rotor and v is the wind speed. However, in practice the extractable power is about half that (one can argue that only one half of the rotor — the scoop co-moving with the wind — works at each instant of time). Thus, one gets $Pmax = (0.18 kgm-3) (\rho.h.d.v^3)$

The angular frequency of a rotor is given by $w = (\lambda . v) / r$, where r is the radius and λ is a dimensionless factor called the tip speed ratio. λ is a characteristic of each specific windmill, and for a Savonius rotor λ is typically around unity.

For example, an oil-barrel sized Savonius rotor with h=1 m and r=0.5 m under a wind of v=10 m/s, will generate a maximum power of 180 W and a maximum angular speed of 20 rad/s (190 revolutions per minute).

In most countries, numerous steam power plants driven by fossil fuels like oil, coal, and natural gas or by other energy resources like uranium are in service today. During the past decades, many power generation companies have paid attention to process improvement in steam power plants by taking measures to improve the plant efficiencies and to minimize the environmental impact (e.g., by reducing the emissions of major air pollutants such as CO2, SO2, and NOx). Exergy analysis is a useful tool in such efforts.[14]

1.9.1 Tip Speed Ratio:

The tip-speed ratio, λ , or TSR for wind turbines is the ratio between the tangential speed of the tip of a blade and the actual speed of the wind. The tip-speed ratio is related to efficiency, with the optimum varying with blade design. Higher tip speeds result in higher noise levels and require stronger blades due to larger centrifugal forces.

 λ = tip speed of blade/wind speed

The tip speed of the blade can be calculated as w times R, where w is the rotational speed of the rotor in radians/second, and R is the rotor radius in metres. Therefore, we can also write:

$$\lambda = wr/v$$

Where v is the wind speed in metres/second at the height of the blade hub.

According to the U.S. Energy Information Administration, the average U.S. home uses 867 kilowatt-hours (kWh) per month. The mean turbine capacity in the U.S. Wind Turbine Database (USWTDB) is 1.67 megawatts (MW). At a 33% capacity factor, that average turbine would generate over 402,000 kWh per month - enough for over 460 average U.S. homes. To put it another way, the average wind turbine generates enough energy in 94 minutes to power an average U.S. home for one month.[15]

1.9.2 Power Coefficient (Cp) Analysis:

Power coefficient (Cp) of a wind turbine is the ratio of maximum power obtained from the wind to the total power available in the wind. This hypothesis shows the relationship between the power coefficient (Cp) and the wind speed (V), which expresses the basic theory of the Savonius wind turbine. Principally the power that the savonius rotor can extract from the wind (Pw) is less than the actual available from the wind power (Pa). The available power (Pa), which is also the kinetic energy (KE) of the wind, can be defined as:

$$KE = Pa = 1/2 \ ma \ . \ V^2 \ (Watt)$$

$$Pa = 1/2 \rho . As . V^3$$
 (Watt)

Where: ma = wind mass flow rate striking the swept area of the wind turbine (kg/sec).

But, the swept area (As = H * D), therefore the actual power becomes:

$$Pa = 1/2 \rho . H . D . V 3$$

The power that the rotor extracts from the wind is:

$$Pw = T * \omega$$
 (Watt)

Where: Pw = the power that the rotor extracts from the wind (Watt).

The power coefficient (Cp) is given by:

Cp = the extracted power from the wind/ the available power of the wind

= **Pw**/

Pa [15]

1.9.3 Relation between wind speed & (rpm ,power):

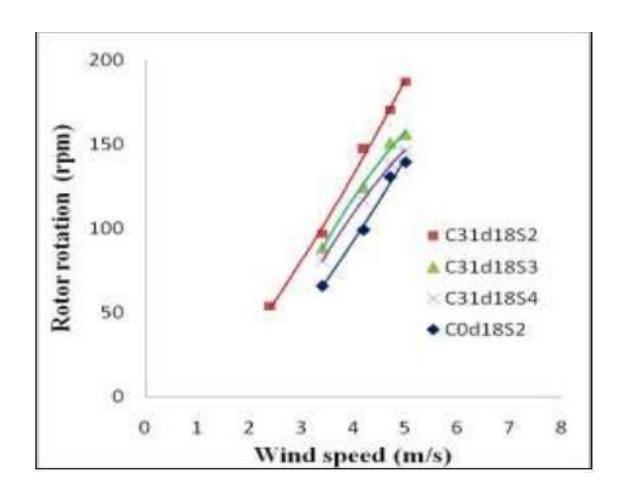


Figure 1-16: Relation between wind speed and rpm

Figure 1 shows the effect of wind concentrator on the rotor speed. The rotor speed depends on the wind velocity. As the wind velocity increases, the rotor rotation elevates. One interesting thing in Figure 1 is the effect of the blade number on the rotor speed. Increasing the number of the blade even decreases the rotor speed. The turbine with two blades results in higher rotor speed than that of more than 2 blades.

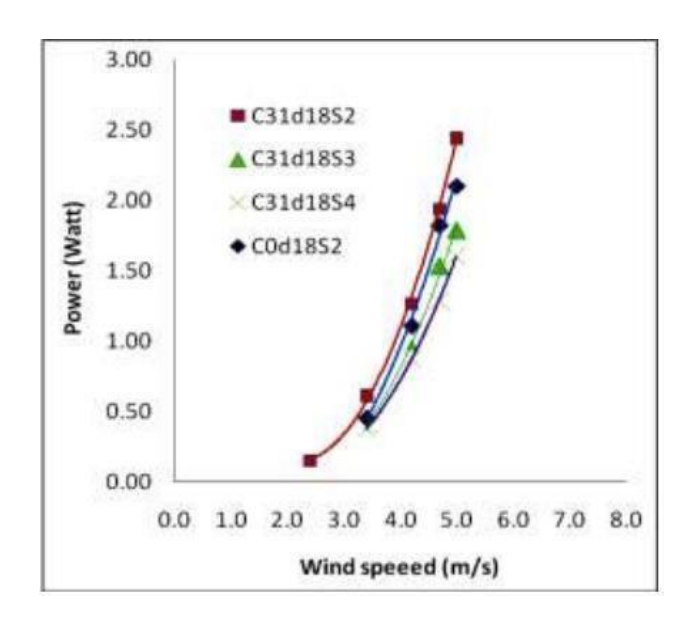


Figure 1-17: Relation between wind speed and power

Similar to the rotor speed, the power also increases with the increase in the wind velocity, see Figure 2. As the number of the blade is increased, the power of the turbine even declines. In Figure 1, although the rotor rotation decreases with the blade number, but the rotor rotation is still higher than that of the wind turbine without a concentrator. Meanwhile, in Figure 2, the turbine with 3 and 4 blades results in the lower power than that of the turbine without a wind concentrator. Then this is not suggested to use blades of more than 2 when the turbine is equipped with a wind concentrator [16]

CHAPTER TWO THEORETICAL MODELLING

2.1 Part useful information

Fr= resisting wind force to rotation

Fw=wind force

A=swept area of blades

V= wind velocity

r= rotor redius

D=rotor diameter

d = shaft diameter

H=height

$$D=(2*r)*-d=(2*0.63)-0.01=1.25m$$

Fw= air density*A*v^2 = 1.225*1.5*6^2= 55.12N

2.1.1Blade width

M =blade mass

Density of the blade= 2700

Volume of the blade = (2*1)* thickness

G =gravitational acceleration (9.8m/s^2)

Fg= m*g

M= density of the blade * volume of the blade = 2700*(2*1)*5/1000 = 27 kg

Fg=264.6 N

2.1.2 Tip speed ratio (tsr)

Tip speed ratio = V rotor / V wind = w*r / V wind

2.1.3 Power and torque from blades

Pa = total available power from the wind

Pt = max power obtained from the wind

T = actual rotor torque

Pa= ½ * density * A* v^3

Pt = T *W

Cp= pt/pa <1

Cp max = 0.59

2.1.4 Betz law

Tw = theoretical torque

Cm= T/Tw

Tw=1/4*density * A* r * v^2= 1/4 *1.225*1.25* 0.63*6^2= 8.68 N.m

Cp and Cm play major role in identifying the effeincy of VAWT

2.2 Force analysis on the turbine parts

fw= wind force

fg=blade weight

fc= centrigal force due to rotation

fc=
$$m*v^2/r = 27 * 6^2 / 0.62 = 1542.8 N$$

Tw= Fw*
$$r/2$$
 - Fr * $r/2$ = $\frac{1}{4}$ * density *A *r* v^2 = 8.68 N.m

Fr= 27.56 N Fw = 55.12N r= 0.63 m Fc= 1542.8 N Fg= 264.6N

2.3 stress analysis

2.3.1 Stresses on turbine blades rodes

Direct shear due to centfugal

Ar= rod rea = $\pi/4 * dr^2$

Syr= yield for the rod material = 240 *10^6

sr= factor of safty for the rod = 2

Shear =
$$Fc/2*Ar = 0.5*Syr/Fsr$$

$$1542.8/(2*\pi/4*dr^2) = 0.5*240*10^6/2$$

$$dr = 4.04*10^{-3} m$$

2.3.2direct shear due to weight

shear =
$$Fg/2*Ar = 0.5*Syr/Fsr$$

$$dr = 8.4 *10^{-4}$$

2.3.3torsion due to weight (Fg)

$$L=(r/2 - a)$$

Shear=
$$T*dr/(2*\pi/32*dr^4) = 0.5*Syr / fsr$$

dr =

2.3.4. Compression stress due to wind forces

$$\sigma c = \frac{\frac{fw-fr}{2}}{2} = \frac{Syr}{2}Fsr = \frac{241}{2}2 = 120.5 * 10^6 N/M^2$$

Ar : Rod area = π / 4 dr^2

$$dr3 = \frac{\sqrt{2(Fw - Fr)fsr}}{\pi Syr} = \sqrt{2(54.46 - 27.21) * 2 \pi * 241} = 0.389$$

2.3.5. Material selection for the blades

Blades need to be light for the air to be able to push them, so steel can't be used as a material for them. Hence forward aluminum will be used as blades material as its density is smaller and yield strength is higher than that of steel.

 ρ aluminum = 2700 kg/m3.

Syb: Yield stress of blades = 276 MPa.

fsb: Factor of safety of blades = 3

2.3.6 Tension stress due to centrifugal force:

$$\sigma T = \frac{Fc}{Af} = \frac{Syb}{Fsb} = \frac{273}{3} = 92 * 10^6$$
 N/M

Af: Tension area = $H * t - 2dr * t = 8.385*10^{-6} m^{2}$.

t: Blade thickness (mm).

 \therefore t = 8.385 1000-(2*20) = 8.73 * 10-3 mm.

: t < 5 mm (then it is safe for the blade thickness).

2.3.7. Bending stress due to weight:

$$\sigma b = \frac{My}{Ib} = \frac{Syb}{fsb} = \frac{276}{3} = 92 * 10^6 N/M^2$$

y: Distance from blade center to its edge = H/2 = 1000/2 = 0.5 M

t: Blade thickness = 5 mm.

H: Blade height = 1 m.

M: Bending moment = Fg I = Fg (r/2 - a) = 132.43 (630/2 - 5) = 41053.3 N. mm.

Ib: Moment of inertia = $(t*H^3/12) - (2*t*dr^3/12) = 148743.84 \text{ mm4}$.

$$(t*1000^3/12) - (2*t*20^3/12) = 148743.84$$

∴ t = 1.78 * 10^-3 mm

t < 5 mm (then it is safe for blade thickness).

2.3.8. Direct shear due to weight

$$\tau c = \frac{Fc}{4Al} = \frac{0.5Syb}{fsb} = \frac{0.5*276}{3} = 46 * 10^6 N/M^2$$

Al: Area of shear stress due Fc at blade edge = a*t.

t: Blade thickness = 5 mm

 \therefore a1 = Fgfsb/tSyb = 132.43*3/5*276 = 0.287*10^-3 m

2.3.9:Direct shear due to centrifugal (fc)

$$\tau c = \frac{Fc}{4^*al} = \frac{0.5Syb}{fsb}$$

AL is a shear area =(a*t)

A=π/4 D^2

SY=YIELD FOR ROD MATERIAL

$$\frac{Fc}{4^*(a^*t)} = \frac{0.5Sy}{fsb}$$

We take fsb=3 for blade and t is known

a = 0.005 m

we take a then round it up

2.3.10: Bearing or crushing stress on rod

A: bearing or crushing due to centrifugal (fc)

 $\sigma br = fc/\text{project area} \leq \text{syr/fsr}$

$$\frac{fc}{dr} * t \le \frac{syr}{fsr} = 771.43/20.5 \le 241/2 = 70714 \le 120.5$$

If left side≤ right side (Dimenstions of dr and t are suitable for design)

B: bearing due to weight (fg)

$$\sigma b$$
r = $\frac{fg}{projectarea} \le \frac{syr}{fsr}$

$$\frac{fg}{dr} * t \le \frac{syr}{fsr} = \frac{132043}{20.5} \le \frac{241}{2} = 1.324 \le 120.5$$

If left side≤ right side

Dimenstions of dr and t are suitable for design.

Final dimensions are: dr =0.02m, t=0.005, a=0.005m

2.4 Design of Shaft

A shaft is a rotating member, usually of circular cross section, used to transmit power or motion. It provides the axis of rotation, or oscillation, of elements such as gears, pulleys, flywheels, cranks, sprockets. There is really nothing unique about a shaft that requires any special treatment beyond the basic methods already developed in previous chapters. However, because of the ubiquity of the shaft in so many machine design applications, there is some advantage in giving the shaft and its design a closer inspection.

Details of the shaft itself will be examined, including the following:

- 1. Material selection
- 2. Geometric layout
- 3. Stress and strength
- 4. Static strength
- 5. Fatigue strength
- 6. Deflection and rigidity
- 7. Bending deflection
- 8. Torsional deflection

2.4.1 Shaft Materials

Deflection is not affected by strength, but rather by stiffness as represented by the modulus of

elasticity, which is essentially constant for all steels. For that reason, rigidity cannot be controlled by material decisions, but only by geometric decisions. Necessary strength to resist loading stresses affects the choice of materials and their treatments. Many shafts are made from low carbon, cold-drawn or hot-rolled steel. Significant strengthening from heat treatment and high alloy content are often not warranted. Fatigue failure is reduced moderately by increase in strength, and then only to a certain level before adverse effects in endurance limit and notch sensitivity begin to counteract the benefits of higher strength. A

good practice is to start with an inexpensive, low or medium carbon steel for the first time through the design calculations.

It means to find the suitable diameter to sustain the previous eight problem face the shaft.

	s of Shafting N			Sy	Sy MPa			
Material	Percent Carbon	Tension	Compression	Shear	Tension	Compression	Shear	Elongation
Commercial: Cold-rolled	0.10 — 0.25 0.10 — 0.25	483	483	241 207	241	241	124	-35 35
Commercial: Hot rolled or forged	0.15 — 0.25 0.25 — 0.35 0.35 — 0.45 0.45 — 0.55	483 517 552	414 483 517 552	221 241 255 276	248 276 310 345	248 276 310 345	112 121 129 138	26 24 22 20
3.5 / Nickel	0.15 - 0 25	586	586	293	379	379	147	2 6

In the first step we choose the material of the shaft & from the table of material properties we

get the tensile yield strength and the ultimate strength in MPa (Table 1)

Material chosen: Commercial cold rolled steel (0.1-0.25 %C)

Su= 483 MPa Sy=241 MPa

2.4.2 Design based on Distortion energy theory

$$d^{3} = \frac{16 * f.s}{\pi * S_{y}} \sqrt{4M^{2} + 3T^{2}}$$

d = 9.22 mm

d: The solid shaft diameter (mm)

f.s: Factor of safety of the shaft = 2.5

M: Maximum bending moment in the shaft = 0 N.mm

T: Maximum Torque in the shaft = 8578 N.mm

2.4.3 Design based on Rigidity

$$d \geq \sqrt[4]{\frac{584TL}{G\theta_{all}}}$$

$d = 68.08 \, mm$

T: Torque applied on shaft = 8578 N.mm

L: Length of shaft affected by the torque = 2000 mm

G: Modulus of rigidity = 80000 MPa

Theta all: Allowable shaft twist angle (0.167°/ m for suddenly change in direction)

Theta all = $2(0.167) = 0.334(pi/180) = 5.83x10^{-3}$ radian

2.4.4 Design based on Fatigue loading (Soderberg Equation)

$$d^3 = \frac{32 * f.s}{\pi} \sqrt{\left(\frac{k_f * M}{S_e}\right)^2 + \left(\frac{T}{S_{y_{tension}}}\right)^2}$$

$$\mathbf{k_f} = 1 + \mathbf{q} \left(\mathbf{k_t} - 1 \right)$$

d = 9.68 mm

T= 8578 N.mm

Sy= 241 MPa

F.s = 2.5

M = 0 N.mm

q: Notch sensitivity (Fig.1)

kt : Stress concentration factor (Fig.A-15-11) (always > 1)

Se: Corrected endurance stress (MPa)

$$S_e = k_a * k_b * k_c * k_d * k_e * S'_e$$

 S'_e : The endurance stress (MPa) $S'_e = 0.5 * S_u$ For ($S_u < 1400$ MPa)

ka: Surface factor (Fig. 3)

$$k_b \colon \text{Size factor} \qquad \qquad k_b = \left\{ \begin{array}{ll} 1.24 \, * \, \mathrm{d}^{-0.107} & 2.79 \, \leq \, \mathrm{d} \, \leq \, 51 \, \mathrm{mm} \\ 1.51 \, * \, \mathrm{d}^{-0.157} & 51 \, < \, \mathrm{d} \, \leq \, 254 \, \mathrm{mm} \end{array} \right\}$$

$$k_c : \text{Loading factor} \qquad k_c = \left\{ \begin{aligned} 1 & & \text{Bending loading} \\ 0.85 & & \text{Axial loading} \\ 0.59 & & \text{Pure torsion} \end{aligned} \right\}$$

When torsion is combined with other stresses, such as bending, kc = 1

$$\mathbf{k_d} : \mathsf{Temperature} \; \mathsf{Factor} \qquad \qquad k_d = \left\{ \begin{array}{cc} 1 & \qquad & \mathbf{T} = 20 \; ^{\circ} \mathsf{C} \\ 1.01 & \qquad & \mathbf{T} = 50 \; ^{\circ} \mathsf{C} \end{array} \right\}$$

ke: Reliability Factor (Table 11)

2.4.5 Design based on ASME formula for ductile material

$$d^{3} = \frac{16}{\pi * \tau_{all} (1 - C^{4})} \sqrt{\left(k_{m} * M + \frac{\alpha * F_{a} * d(1 + C^{2})}{8}\right)^{2} + \left(k_{t} * T\right)^{2}}$$

$$C = \frac{d_{i}}{d_{a}}$$

di: Inner shaft diameter

do: Outer shaft diameter

tall: Allowable shear stress

tall = minimum value of [0.3 Sy or 0.18 Su] for no keyway

tall = 0.75*minimum of [0.3 Sy or 0.18 Su] for keyway

km, kt: combined shock and fatigue factors table(12)

Fa: Axial load in shaft (N)

C=0

tall=0.3(241)= 72.3 MPa

tall=0.18(483)= 86.94 MPa

Table (12) Combined Fatigue Factors

Nature of Load	Stationar	y Shaft	Rotating Shaft		
Nature of Load	Km	Kt	Km	Kt	
Gradually applied load, steady	1.00	1.00	1.50	1.00	
Suddenly applied, minor shock	1.5 : 2	1.5 : 2	1.5 : 2	1.0:1.5	
Suddenly applied, heavy shock			2:3	1.5:3	

From table 12: Choose suddenly applied minor shock & rotating shaft so Km=1.5 Kt=1

M=0

 ρ steel = 7800 kg/m3 Fa: axial load = 2Fg + Fsh

Fsh: weight of shaft = $(g)(\rho steel)(Vsh) = 9.81*7800*(1.41x10^(-3)) = 107.89 N$

Vsh= $(pi/4)(d^2)(L)= (pi/4)(0.03^2)(2)= 1.41x10^(-3) m3$

Fa= 2(132.43)+ 107.89= 372.75 N

d = 30 mm = 0.03 m

 α : column action factor (buckling action)

- o Tensile Load (α=1)
- o Compression load

$$\alpha = \frac{1}{1 - 0.0044 \left(\frac{L}{k}\right)} \qquad \text{if} \quad \frac{L}{k} \le 115$$

$$\alpha = \frac{S_y}{\pi^2 * n * E} \left(\frac{L}{k}\right)^2 \qquad \text{if} \quad \frac{L}{k} > 115$$

$$\alpha = \frac{S_y}{\pi^2 * n * E} \left(\frac{L}{k}\right)^2 \quad \text{if} \quad \frac{L}{k} > 11$$

 $k=\sqrt{\frac{I}{A}}$ Gyration ratio (no physical meaning) (mm)

 $I = \frac{\pi}{64} d^4$ I : moment of inertia of the shaft cross section (mm⁴)

A: cross-section area of the shaft (mm²)

n: fixation factor (n = 1.6) for bearing fixation

E : modulus of elasticity (MPa) E = 200 GPa

Compression load:

d= 30 mm

I=39760.78202 mm4

A=706.8583471 mm2

K=7.5

L/K = 2000/7.5= 266.67 > 115

Sy=241 MPa

 $\alpha = 5.426$

<u>d= 9.31 mm</u>

Diameters = (9.22, 68.08, 9.68, 9.31) mm

Choose 68.08 as it is the biggest diameter

2.5 Selection of bearing

2.5.1 Reaction Calculations on bearing

Fa= Axial load

Fw=55.12 N

FR=27.56 N

Fg= 264.6 N

Weight of shaft = 108.17

Fa= 2*Fg+Weight of shaft

Fa= 2*264.5+ 108.17= 637.374 N



$$R_{B_{x}} = 0.5 * Fa = 318.68 N$$

$$\sum Fy = 0$$

(Fw+FR) =
$$R_{B_y}$$
 82. 68 N

Therefore, Fa =
$$R_{B_x}$$
= 318.68 N

And Fr =
$$R_{B_y}$$
 = 82.68 N

2.5.2 Static Load bearing (C_{or})

$$C_{or} = F_{s} \times P_{o}$$

 F_s : Permissible Static Load Factor = 1.5 (Table 13)

 \boldsymbol{P}_o : Equivalent static bearing load, (N).

Table (13) Permissible Static Load Factor fs

Oneveting Conditions	Lower Limit of fs			
Operating Conditions	Ball Bearings	Roller Bearings		
Low-noise applications	2	3		
Bearings subjected to vibration and shock loads	1.5	2		
Standard operating conditions	1	1.5		

Since,
$$\frac{Fa}{Fr} = 3.8 > 0.8$$
 therefore,

$$P_{_{0}} = 0.6 * Fr + 0.5 * Fa = 208.948 N$$

Where:

Fr: Radial load, (N).

Fa: Axial load, (N)

Therefore,,
$$C_{or} = 313.422 < C_{or_{catalogue}}$$
 (3650)

2.5.3 Check for dynamic load

<u>Γable (16) Calculation factors for single row deep groove ball beari</u>

F _a /C _o	F _a /C _o e		$\frac{F_a}{F_r} \leq e$		$\frac{F_a}{F_r} > e$	
		X	Y	X	Y	
0.014	0.19	1	0	0.56	2.3	
0.025	0.22	1	0	0.56	1.99	
0.04	0.24	1	0	0.56	1.8	
0.056	0.26	1	0	0.56	1.71	
0.07	0.27	1	0	0.56	1.6	
0.084	0.28	1	0	0.56	1.55	
0.11	0.3	1	0	0.56	1.45	

$$\frac{Fa}{C_{or}} = \frac{318.68}{3650} = 0.087$$

$$\frac{Fa}{Fr} = 3.8 > e$$

Therefore, P = X * Fr + Y * Fa = 508.38 N

Where X= 0.56, Y= 1.45

2.5.4 Dynamic Load calculation

$$C = \frac{K_s * P * (L)^{\frac{1}{\epsilon}}}{a_d}$$

Where:

C: Dynamic bearing load, (N).

 $K_{_S}$: Service factor "From table (14)" (assume Light shock =1.5)

L: Life time, (millions of revolutions).

Table (14) Service factor, Ks:

Types of service	Ball bearing	Roller bearing
Uniform and steady load	1.0	1.0
Light shock load	1.5	1.0
Moderate shock load	2.0	1.3
Heavy shock load	2.5	1.7
Extreme shock load	3.0	2.0

$$L=a_L * L_{10} = 1 * 108 = 108$$

 $a_{_L}$: Life-adjustment reliability factor "From table (15)".

 L_{10} : Rating life in millions of revolutions.

Where,
$$L_{10} = \frac{\textit{Operating hours*}3600*n_{r,p,s}}{10^6} = \frac{20000*31600*1.5}{10^6} = 108$$

 a_d : Load-adjustment reliability factor "From table (15)".

ε: constant (depends on kind of bearing)

E = 3 For ball bearing

Table (15) Reliability adjustment factors

Reliability%	Life adjustment Reliability factor	Load adjustment Reliability factor a _D	
	$\mathbf{a_L}$	Roller bearing	Ball bearing
90.0	1	1	1

therefore,,

$$C = \frac{1.5*508.38*(L)^{\frac{1}{3}}}{1} = 3631.51$$

Therefore

Dynamic load
$$C_{catalogue} > C$$
 (4700>3631.51)

So, Bearing 6806 zz is selected

CHAPTER THREE EXPERIMENTAL METHOD

3.1 EXPERIMENTAL STUDY:

In the present work, the experimental study will be carried out in two main experiments, the first set of experiment study the bearing friction force and aerodynamics drag effect produced by traditional Savonius blades and modified Savonius blades at various wind speed, the second set of experiment are carried out to measure the static torque produced by Savonius blade rotor for different angular position at various wind speeds. The experiments are made for both traditional and modified Savonius blade rotor. The torque value may be estimated using the brake drum measuring system or using torque sensor.

3.2 EXPERIMENTAL SETUP:

The experimental setup included a structural test bench with the Savonius wind rotor, measuring devices, and a wind tunnel. The wind tunnel used in the studies was an open circuit tube with a circular exit section with a diameter of 70 cm. An adjustable damper might also be used to vary the wind velocity downstream of the exit section. Figure 4.1 depicts a schematic diagram of the experiment setup that was employed in this investigation.

Due to the lack of space downstream of the wind tunnel exit from the laboratory, the Savonuis wind rotor was located roughly I = 5 m away from the wind tunnel exit in order to produce a homogeneous air flow. Due to a lack of space downstream of the wind tunnel exit from the laboratory, a set of screens was used to provide a uniform air flow, and the wind rotor was placed at a distance of 1 m measured from the last screen. The set of screens consists of three screens with a grid of 10mm10mm and a distance of 120 mm between the first, second, and third screes. To reduce friction torque, the savonuis rotor shaft is supported by two very low friction bearings in a cantilever arrangement (moment). The use of bolts and nuts allowed for easy rotor replacement of various types. A pitot static tube linked to a manometer measures the wind velocity. A brake drum (pulley) dynamometer is used for loading the Savonius rotor. A fishing nylon thread with a diameter of 1 mm connects a beam type load cell and a digital reading weighted balance. If the torque of the rotating Savonius rotor friction in the bearing and the 1 mm nylon wire string coiled of the rotor shaft must be decreased, friction is an essential parameter that affects the measurements. Before mounting the bearing, the seals were removed and the bearing rinsed in petrol to remove the grease, resulting in reduced friction.

The rotor is allowed to rotate at no load speed when the wind velocity is regulated to a certain Reynold number. A speed sensor of type DC5V-24V 600P/R measures the rotor's rotating speed. Before each reading, each bearing is sprayed with W-D 40 (a commercially available spray) lubricant. The rotor is gradually loaded to record weight balance, load cell data, ForcesF1, F2, and rotor rotational speed. Using the brake drum measuring system, a series of tests are carried out to evaluate the static torque of the rotor at a certain rotor angle. The static torque of the rotor is measured at every 15° of the rotor angle. The inclusion of a worm gear box simplified the rotor loading process. Acquired and managed at a specific wind speed to inhibit spinning from a given rotor angle, the rotor is weighted. The static torque at a given rotor angle is calculated using the load (F1) and spring balance (F2) data.

Readings are used to calculate the static torque at a given rotor angle as: TR = (F1 - F2) g (Dpully + Dwire) / 2 Where TR is loading moment of the rotor (static torque) in N.mm F1 is the force in the tight side of nylon wire attached to the beam type load cell in kg. F2 is the force in the slack side of nylon wire attached to the digital spring balance in kg. Dpulley is 40 mm& the diameter of the nylon wire in mm (Dwire = 1 mm). g is the gravity in m/s2 (g = 9.81 m/s2). More detailed information about the equipment's that are going to be used and described in the following section.



Figure 3.1. Experimental setup.

3.3 EQUIPMENT:

The equipment's to be used are the subsonic wind tunnel of open return type, pitot static probe, load cell of beam type to measure the tensile force in the highest side of the nylon string, torque sensor, weight balance to measure the tensile force in the slack side of the nylon string a support structure and CPU unit.

3.3.1 Wind Tunnel

The Hampden Model H-6910-12-150-CDL wind tunnel is equipped with the basic facilities or generating air flows which are used in the experiment. The wind tunnel including an inlet cone, clear experiment section of 30 * 30 CM, outlet cone with a blower fan and a main AC circuit breaker.

3.3.2 Pitot Static Probe

Pitot static tube of a modified Prandtl type is used to measure the total and static pressure at the same point in air moving air stream in the test section at the downstream move there

wind tunnel the years stream velocity maybe calculated it using the following relation v=4.039 $\sqrt{\Delta}L$ Where is V is the air velocity.[25

3.3.3 Load Cell:

The load cell may be used to measure the force F1 in tight side of the nylon string in kg. The load cell was selected as a beam type of 20 kg constructed in a cantilever beam serves as the elastic member to measure the force F1 acting on the tight side of the nylon string. Two strain gauges on the top surface and strain gauges on the bottom surface (all oriented along the axis of the beam) act as the sensor. The gages are connected into a Wheatstone bridge as shown in the figures (4.2- 4.3)



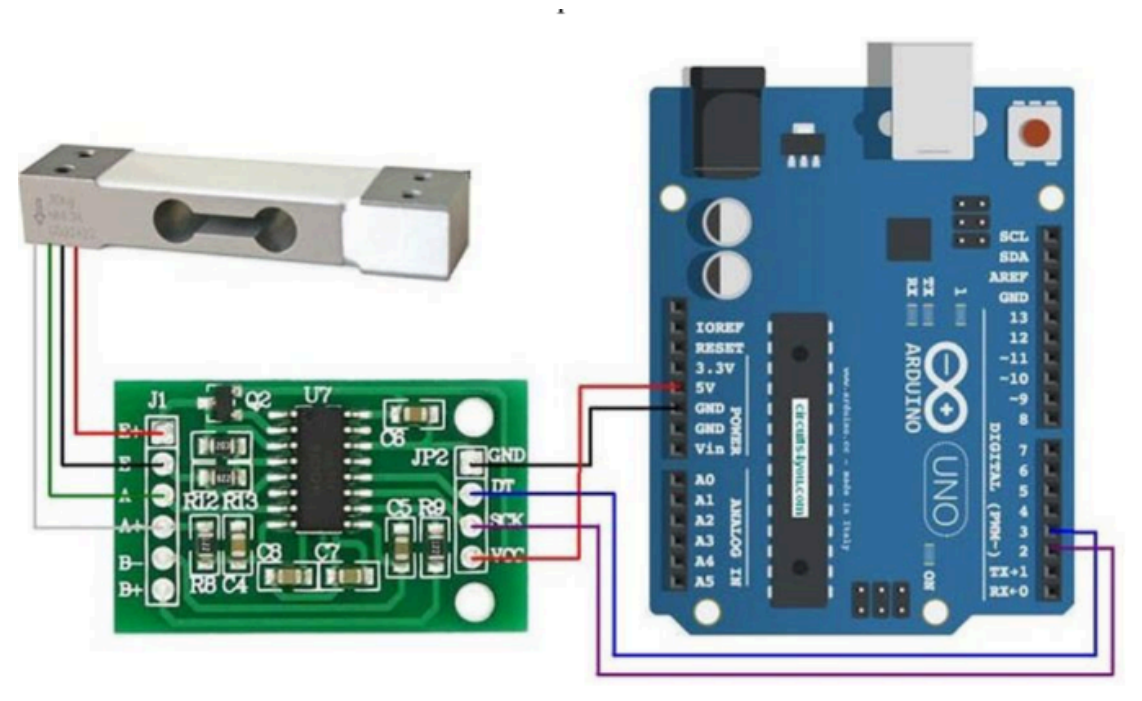
Figure 3.2. Load Cell. [26]

3.3.4 Arduino

The Arduino is introduced to covers HX711 Load Cell amplifier interface. We are interfacing a 20 Kg load cell to the Arduino using HX711 load cell. HX711 is a precision 24-bit analog to-digital converter (ADC) designed for weigh scales and industrial control applications to interface directly with a bridge sensor. The input multiplexer selects either Channel A or B differential input to the low-noise programmable gain amplifier (PGA). Channel A can be programmed with a gain of 128 or 64, corresponding to a full-scale differential input voltage of ±20mV or ±40mV respectively, when a 5V supply is connected to AVDD analog power supply pin. Channel B has a fixed gain of 32. On chip power supply regulator eliminates the need for an external supply regulator to provide analog power for the ADC and the sensor.

Clock input is flexible. It can be from an external clock source, a crystal, or the on-chip oscillator that does not require any external component. On-chip power on-reset circuitry simplifies digital interface initialization. There is no programming needed for the internal

registers. All controls to the HX711 are through the pins. Figure 4.4. Shows the wiring



between the load cell and the Arduino and amplifier.

Figure 3.3 The wiring with load cell, amplifier & Arduino

3.3 Turbine Manufacturing and Design:

3.3.1 Blades Design:

Because the blades are such an important component of the Savonius turbine, the dimensions of the blades were determined using research and literature surveys [11-14]. For example, the height of the blades was set at 200 mm, and the width was set at 314 mm with an extra 10 mm to glue the blade to the shaft, and when the blades were twisted into a c shape, the diameter was set at 200 mm, and the aspect ratio was set at 1 (aspect ratio: the ratio between height and width). Also, to avoid affecting the Savonius rotor's performance by preventing air from passing through and shutting the gate from behind, and to analyze simply the effect of the gates, set the overlap to 0. Finally, these dimensions were applied to the solid works. As we mentioned earlier, we will work on two types of blades, the first will be old design and the second one will be the new design using additional artilon pieces.

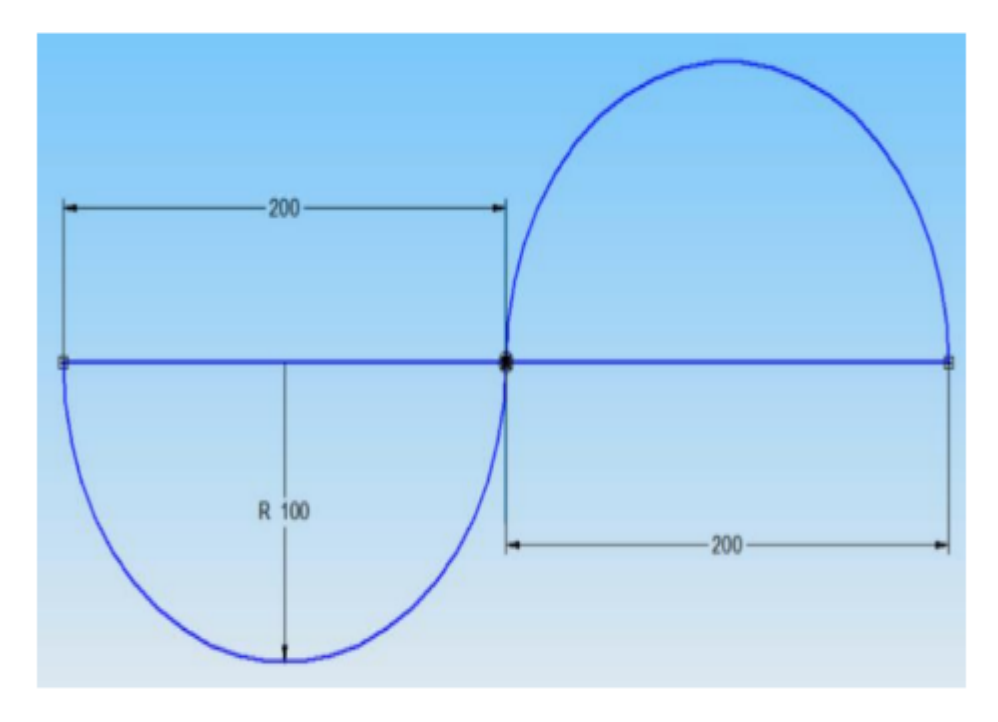


Figure 3.4 Blades Top View

3.3.2 Shaft Design:

It is a hollow shaft made of aluminum, its length is 280 mm this length includes 200 mm blade height and 50 mm for safety and 30 mm installed in the artylon piece which has a diameter from one side is 25 mm and from the other side is 17 mm, and the thickness of shaft is 2 mm and the outside diameter is 19 mm and the inside diameter is 17 mm.

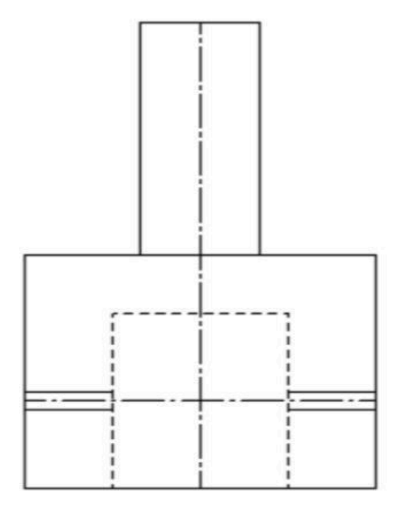


Figure 3.5 Design of Artylon coupling

Figures (3.6-3.7-3.8-3.9-3.10) introduced a photo to describe the whole components used in the experimental set



- 1-Outlet of wind tunnel.
- 2-Wooden frame.

Figure 3.6 Wind Tunnel Setup



Figure 3.7 Thermo Anemometer

Thermo Anemometer is used to measure air velocity coming from the wind tunnel.



Figure 3.8 Image of the electric panel of the setup

- 1- Display set of torque sensor
- 2- Circuit breaker
- 3- 24V power supply
- 4- Amplifier
- 5- 12V power supply
- 6- Arduino board

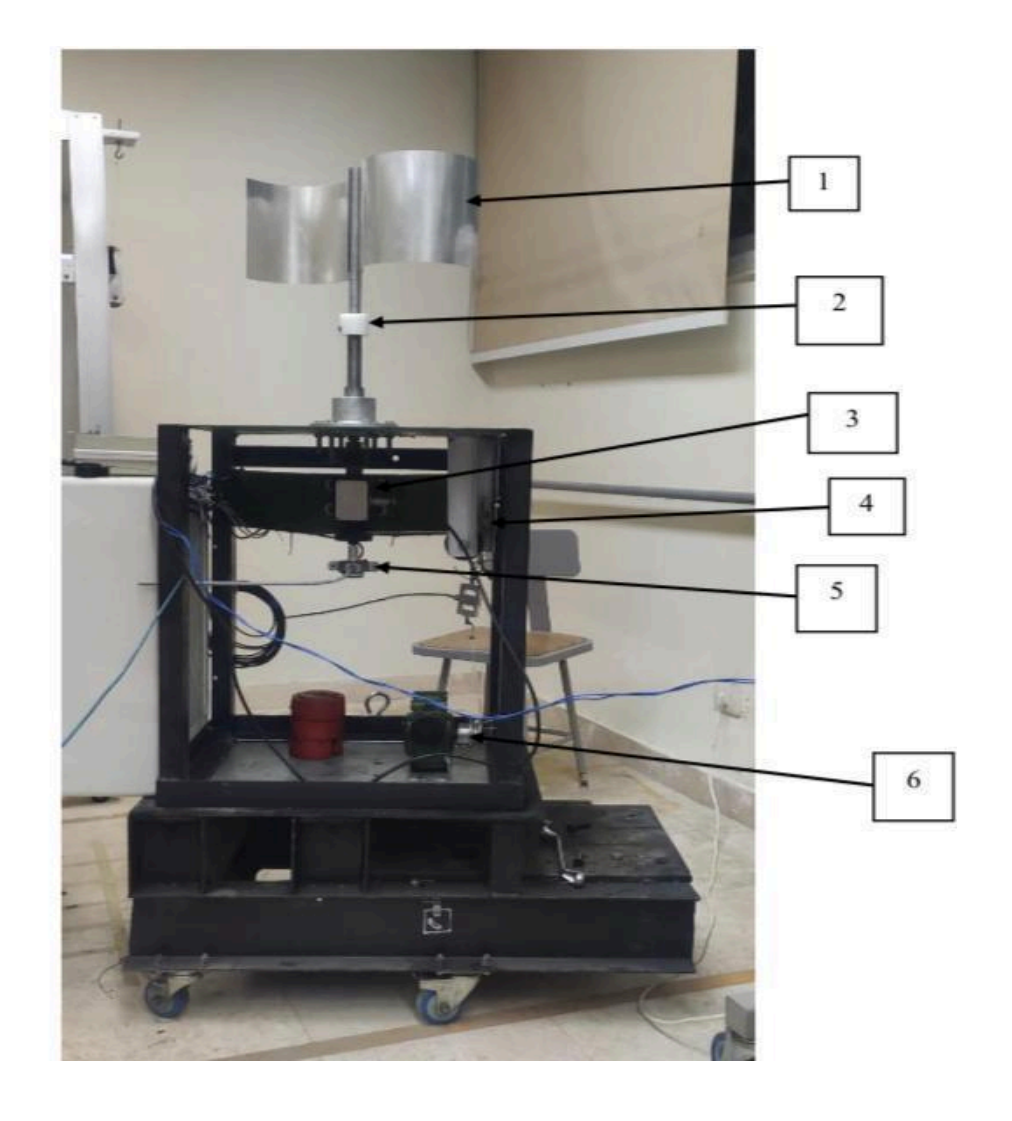


Figure 3.9. Side view of the old design

- 1- Blades
- 2- Artylon Coupling
- 3- Dynamic torque sensor
- 4- Load cell
- 5- Speed Sensor
- 6- Worm gear configuration

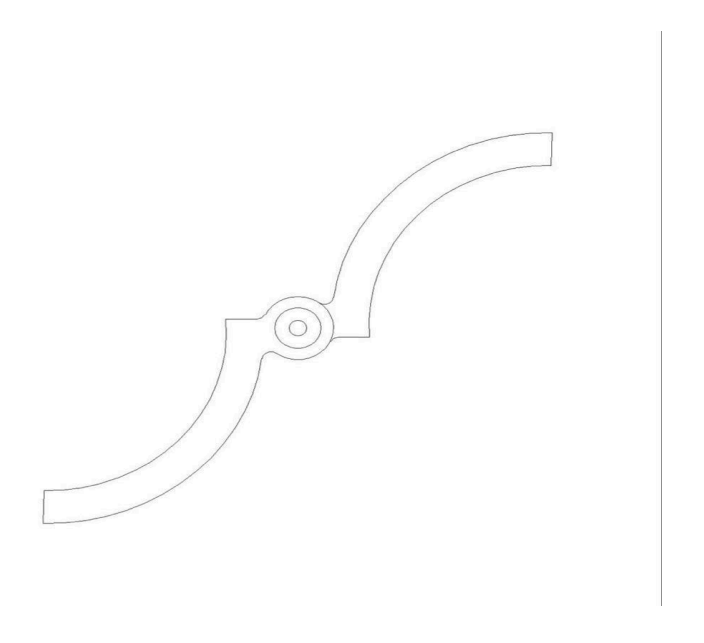


3.3.3 Additional Artilon Design:

The new design requires additional artilon pieces which are 4 pieces of part 1 and 1 piece of part 2 as shown in the following figures



Figure 3.11 Artylon part 1



3.4 Data Reduction:

1- Reynold number based on the rotor diameter is given by: $Re = \frac{\rho V \infty D}{\mu}$

V ∞ is the free stream velocity. D is the rotor diameter (D=200 mm) and μ is the absolute Viscosity of air μ =1.825*10-5 at 200 C.

2- Tip speed ratio is given by: TSR= $\frac{wD}{2V\infty}$

Where w is the angular velocity of the rotor.

3- Torque calculated from the measure loads F1 and F2 as mentioned in equation 1 as:

$$T=g(F1-F2)(\frac{\textit{Dpulley-Dwire}}{2}) * 10^{-3}$$

Where TR is the torque in N.m.

4- Coefficient of torque Ct, coefficient of static torque Cts and coefficient of power Cp given

by: Ct=
$$\frac{4T}{\rho V \infty^2 D^2 H}$$

$$Cts = \frac{4Ts}{\rho V \infty^2 D^2 H}$$

$$Cp = TSR \times Ct$$

5- Balance ratio (B) is given by: $B = \frac{HD}{Aexit}$

Where Aexit is the area of the wind tunnel exit section the effect of blockage ratio is negligible

On Cp ,Ct and Cts for rotor are open jet wind tunnel as reported by Kemoji [24]; in the present

study blockage ratio is negligible where the tests are carried out in the downstream of the wind tunnel exit section. H and D are the height and the diameter of the rotor.

6- Aspect ratio:
$$\gamma = \frac{H}{D}$$

Where in the present study aspect ratio = 1 where H =D =200 mm

3.5 EXPERIMENTS:

3.5.1 Experiment 1 : Static torque, RPM, Power produced by Savonius rotor for different angular position at various wind speed:

Experiment was carried out to evaluate the static torque,RPM,power produced by traditional and modified Savonius rotor for different angular position at every 30° Of the rotor angle at

various value of wind speed.

Test Procedure:

- 1- Adjust the rotor blades to be at the specified position 0,30,60,90,120,150 and 180.
- 2- Rotate the worm to increase the forces F1 and F2and then loading the rotor of the turbine

loading the break drum measuring system until the force f4 reach a value about 5 Kg.

3- Start the wind tunnel and adjust the speed of the fan to obtain the required value of the air

velocity at downstream from the wind tunnel exit section.

4- Use the pitot static tube which attached to the inclined manometer to measure the velocity

of the free air stream up stream of the rotor position.

- 5- Make a fine turning for the fan speed to get the desired value of the free air velocity.
- 6- Release the loading of the brake down system by ready the worm gradually in the c.c.w direction till the rotor start to move.
- 7- Make a fine turning for the motion of the worm to obtain the condition for static torque.
- 8- Record the value of F1 (load cell) and F2 (weight balance).
- 9- Determine the value of static torque using the relation (4) as:

Ts =
$$(F1 - F2)*g*(Dpulley-Dwire)/2*(1/1000)$$

- 10- Determine the value of rpm of rotor
- 11- Calculate the power by multiplying torque by RPM

Repeat the experiment from different angular position at various wind speeds. Coefficient of static torque is obtained is for rotor angles ranging from 0 to 360 in step of 30.

CHAPTER FOUR RESULTS AND DISCUSSION

4.1 New Design Results

Table 4.1 New Design Results

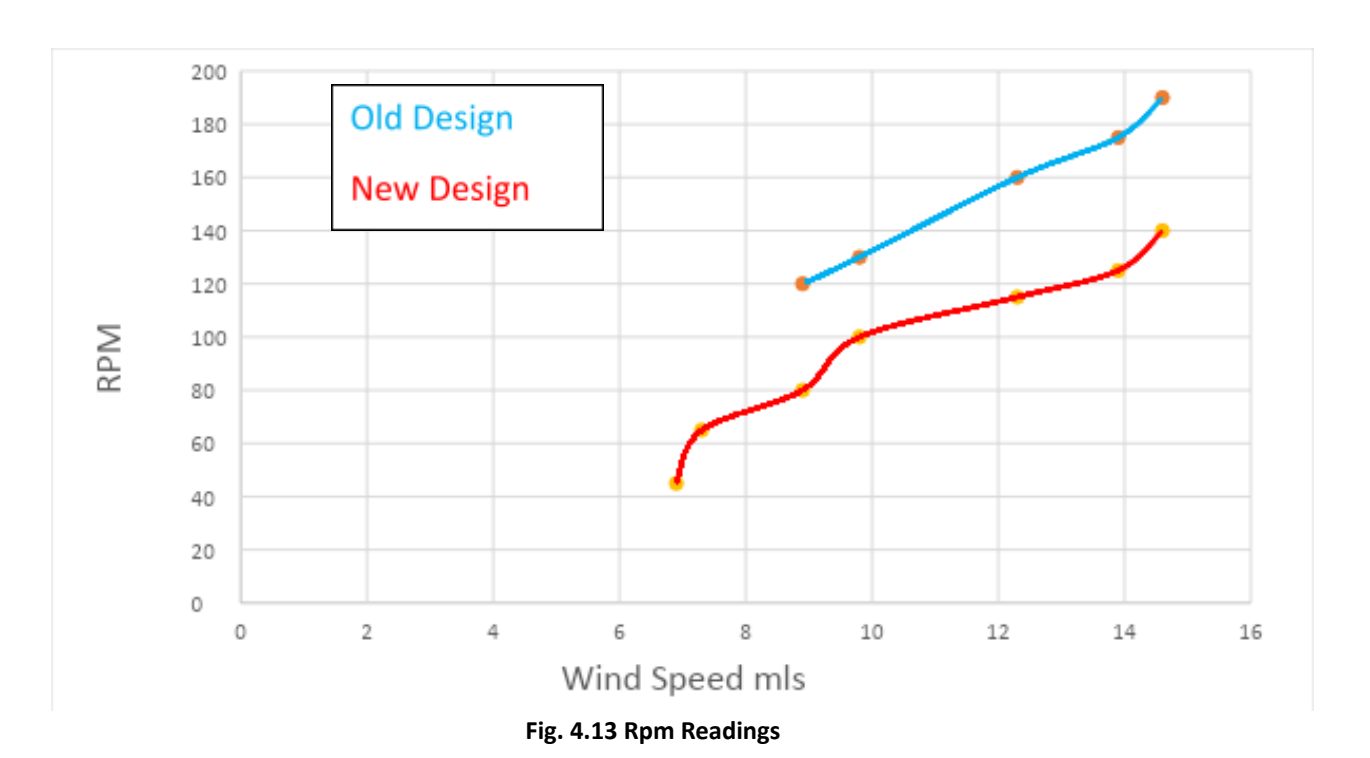
Time (s)	V (mls)	Tunnel RPM	RPM	T +ve	T -ve	T (Nm)	Power (W)
0-40	6.9	1700	45	0.006	-0.004	0.01	0.0471
40-75	7.3	1900	65	0.006	-0.012	0.018	0.12246
75-110	8.9	2100	80	0.006	-0.019	0.025	0.209333
110-160	9.8	2300	100	0.006	-0.024	0.03	0.314
160-225	12.3	2500	115	0.007	-0.031	0.038	0.457393
225-260	13.9	2700	125	0.007	-0.034	0.041	0.536417
260-300	14.6	3000	140	0.007	-0.043	0.05	0.732667

4.2 Traditional Design Results

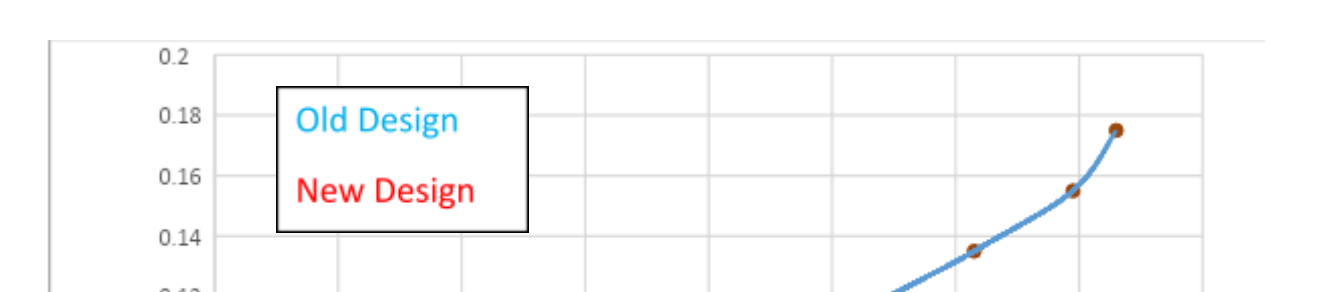
Table 4.2 Traditional Design Results

Time	V (mls)	Tunnel RPM	RPM	T +ve	T -ve	T (Nm)	Power (W)
250-300	8.9	2100	120	0.02	-0.05	0.07	0.8792
350-400	9.8	2300	130	0.025	-0.08	0.105	1.4287
450-520	12.3	2500	160	0.025	-0.11	0.135	2.2608
560-650	13.9	2700	175	0.025	-0.13	0.155	2.839083
670-720	14.6	3000	190	0.025	-0.15	0.175	3.480167

4.3 RPM Readings



4.4 Torque Readings



4.5 Power Readings

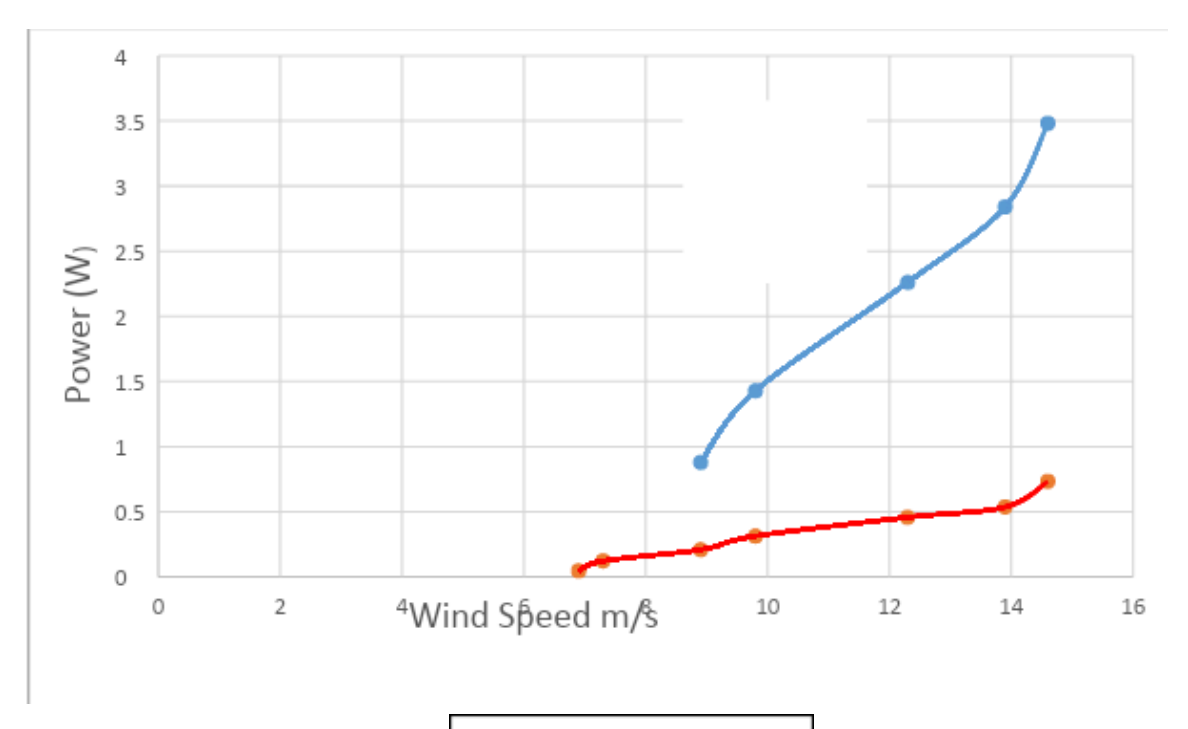


Fig. 4.15 power Readings

Chapter Five

Conclusion

5.1 Conclusion

We followed the same experimental procedure in both cases and it can be concluded that the traditional Savonius turbine produces higher torque and rotates with a higher RPM than the Modified Savonuis turbine so this derives that the traditional design produces more power. This applies at all different speeds of wind coming from the wind tunnel due to instability of the modified turbine

REFERENCES:

- 1- Raciti Castelli, Marco; Englaro, Alessandro; Benini, Ernesto (2011). "The Darrieus wind turbine: Proposal for a new performance prediction model based on CFD"
- 2- https://en.wikipedia.org/wiki/Vertical-axis wind turbine
- **3-**https://www.luvside.de/en/what-is-vawt/

Felix van König (1978). Windenergie in praktischer Nutzung. Pfriemer. ISBN 3-7906-0077-6.

- 4-https://www.researchgate.net/publication/283870348 Overview of Vertical Axis Wind
 Turbine VAWT is one of the Wind Energy Application
- 5- https://www.sciencedirect.com/topics/engineering/rotor-diameter
- 6- https://www.irjet.net/archives/V2/i3/Irjet-v2i3331.pdf
- 7- https://www.green-mechanic.com/2013/03/vertical-axis-wind-turbine-parts.html
- 8- https://iopscience.iop.org/article/10.1088/1757-899X/288/1/012132/pdf
- 9- https://www.sciencedirect.com/science/article/pii/S111001681200049X

10-

https://www.researchgate.net/figure/Photograph-of-VAWT-attached-to-a-communication-tower-from-11 fig1 285650348

11-

https://electricalacademia.com/renewable-energy/vertical-axis-wind-turbine-vawt-working-types-advantages-disadvantages/

12-https://www.researchgate.net/publication/280918046_Influence_of_Blade_Overlap_and_Blade_Angle_on_the_Aerodynamic_Coefficients_in_Vertical_Axis_Swirling_type_Savonius_Wind_Turbine.

- 13-https://www.researchgate.net/publication/322996566_Performance_characteristics_of_the_Savonius_turbine
- 14- https://en.wikipedia.org/wiki/Savonius-wind-turbine. [

15-https://www.researchgate.net/profile/Mirmanto-Mirmanto/publication/316831476_Effect_of_Concentrator_Blade_Diameter_and_Blade_Number_on_the_Savonius_Wind_Turbine_Performance/links/5912ff08a6fdcc963e7ea43e/Effect-of-Concentrator-Blade-Diameter-and_Blade-Number-on-the-Savonius-Wind-Turbine-Performance.pdf.

16-http://citeseerx.ist.psu.edu/viewdoc/download?doi=10.1.1.406.6071&rep=rep1&type=p

17- Design of Icewind's savonius turbine, https://www.researchgate.net/post/How_is_icewind_wind_turbine_blade_design_better_than_savonius_blade_design_18 March 2021.

18- Mahmoud, N.H. & Damp; El-Haroun, Ahm & Damp; Wahba, E. & Damp; Masef, M.H. (2012). An

experimental study on improvement of Savonius rotor performance. Alexandria Engineering Journal. 51. 19–25. 10.1016/j.aej.2012.07.003.

19- R.Pudur and S.Gao, "Performance analysis of Savonius rotor on different aspect ratio for

hydropower generation," ICPDEN 2015.

20- J.V.Akwa and Gi.A.Júnior, "Discussion on the verification of the overlap ratio influence on performance coefficients of a Savonius wind rotor using computational fluid dynamics," 38 (2012) 141e149, 2011.

- 21- Altan, B.D., Atılgan, M. A study on increasing the performance of Savonius wind rotors. J Mech Sci Technol 26, 1493–1499 (2012). https://doi.org/10.1007/s12206-012-0313-y
- 22- Jeon, K. S., Jeong, J. I., Pan, J.-K. & Denny, Ryu, K.-W., 2015. Effects of end plates with

various shapes and sizes on helical Savonius wind turbines. Renewable Energy, Volume 79, pp. 167-176.

23- Tabassum, S. A. & D., 1987. Vertical-axis wind turbine: A modified design.

Applied Energy, 28(1), pp. 59-67.

24- Roy, Sukanta & Djjwal K., 2015. & Djjwal K., 20

two-bladed Savonius-style wind turbine," Applied Energy, Elsevier, vol. 137(C), pages 117-

125.

25- Utomo,I.S, Tjahjana,D.D.D.P & D.D.P & amp; Hadi,S., & amp; quot; Experimental studies of Savonius wind

turbines with variations sizes and fin numbers towards performance" , AIP Conference

Proceedings 1931, 030041 (2018) https://doi.org/10.1063/1.5024100

26- Irabu, Kunio & Emp; amp; Roy, Jitendro. (2007). Characteristics of wind power on Savonius rotor

using a guide-box tunnel. Experimental Thermal and Fluid Science. 32. 580-586. 10.1016/j.expthermflusci.2007.06.008.